PAPER

The effect of Ge precursor on the heteroepitaxy of $Ge_{1-x}Sn_x$ epilayers on a Si (001) substrate

IOP Publishing Semiconductor Science and Technology

Semicond. Sci. Technol. **33** (2018) 034003 (6pp) https://doi.org/10.1088/1361-6641/aa9e7e

The effect of Ge precursor on the heteroepitaxy of $Ge_{1-x}Sn_x$ epilayers on a Si (001) substrate

Pedram Jahandar[1,3], David Weisshaupt[2], Gerard Colston[1], Phil Allred[1], Jorg Schulze[2] and Maksym Myronov[1,3]

[1] University of Warwick, Department of Physics, Coventry, CV4 7AL, United Kingdom
[2] Universität Stuttgart, Institut für Halbleitertechnik (IHT), Pfaffenwaldring 47, D-70569 Stuttgart, Germany

E-mail: P.Jahandar@warwick.ac.uk and M.Myronov@warwick.ac.uk

Received 29 June 2017, revised 27 November 2017
Accepted for publication 30 November 2017
Published 23 February 2018

Abstract

The heteroepitaxial growth of $Ge_{1-x}Sn_x$ on a Si (001) substrate, via a relaxed Ge buffer, has been studied using two commonly available commercial Ge precursors, Germane (GeH_4) and Digermane (Ge_2H_6), by means of chemical vapour deposition at reduced pressures (RP-CVD). Both precursors demonstrate growth of strained and relaxed $Ge_{1-x}Sn_x$ epilayers, however Sn incorporation is significantly higher when using the more reactive Ge_2H_6 precursor. As Ge_2H_6 is significantly more expensive, difficult to handle or store than GeH_4, developing high Sn content epilayers using the latter precursor is of great interest. This study demonstrates the key differences between the two precursors and offers routes to process optimisation which will enable high Sn content alloys at relatively low cost.

Keywords: GeSn, semiconductor, indirect-to-direct bandgap, SiGeSn, $Ge_{1-x}Sn_x$, CVD chemical vapour deposition, GeH_4 germane Ge_2H_6 digermane $SnCl_4$ tintetrachloride

(Some figures may appear in colour only in the online journal)

1. Introduction

Germanium tin ($Ge_{1-x}Sn_x$) is an intriguing semiconductor material for electronics and photonics applications as it undergoes an indirect-to-direct energy bandgap transition for $x \geqslant 0.09$ (over 9% Sn content) [1–5]. This has been shown in recent research [6], however, further research is required to achieve higher growth rate with high enough Sn content with smooth surface (rms $\leqslant$ 1 nm) to reach the indirect-to-direct bandgap transition necessary for high efficiency photonic applications. Nowadays, $Ge_{1-x}Sn_x$ epilayers can be grown not only by research type molecular beam epitaxy, but by industrial type chemical vapour deposition (CVD) directly on silicon (Si) substrate via a relaxed Ge buffer [1, 2, 8, 9]. The growth of high Sn content $Ge_{1-x}Sn_x$ epilayers by CVD opens up a pathway for the commercialisation of devices fabricated from this alloy in a range of photonics applications including light emission and detection. However, reducing the cost and improving impact of incorporating $Ge_{1-x}Sn_x$ into the Si industry will require the availability of relatively low-cost, mass produced and easy to handle/store Ge and Sn precursors. After initial demonstration of CVD growth of $Ge_{1-x}Sn_x$ epilayers over 10 years ago, an interest to this material begun to resurrect [1, 8]. However, many researchers quickly realised that such growth, by the very rare and expensive precursor tin deuteride (SnD_4), is unpractical [1, 2, 8, 10]. The growth of $Ge_{1-x}Sn_x$ was then demonstrated using tin tetrachloride ($SnCl_4$) in combination with Ge_2H_6. [1, 4, 9]. Very promising results have been reported so far with high levels of Sn incorporation, up to ~14%, have been obtained in relaxed $Ge_{1-x}Sn_x$ epilayers [1] including the demonstration of lasing from such material [6, 9, 11]. However, Ge_2H_6 is significantly more expensive than GeH_4, its availability is limited, and its lifetime and stability are

[3] Authors to whom any correspondence should be addressed.

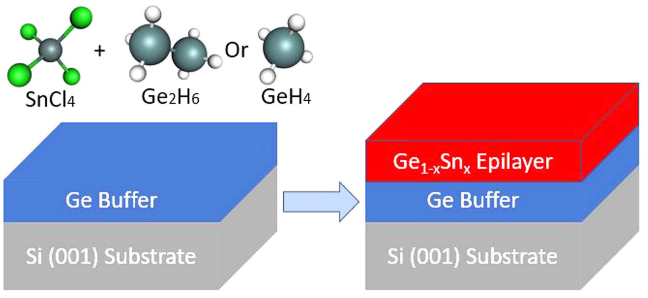

Figure 1. The structure of the layers: the Ge buffer is based on the Si (001) substrate. $SnCl_4$ is used as the source of Sn with H_2 as the its carrier gas. Ge_2H_6 or GeH_4 was used, with constant partial pressure of 10 mTorr and 20 mTorr, respectively. The average thickness of Ge buffer layer is ~1.2 μm.

questionable. Due to this, there is enormous interest from both academic and industrial research communities to replace Ge_2H_6 with an alternative Ge precursor to grow $Ge_{1-x}Sn_x$ epilayers. The GeH_4 is widely used in the semiconductor industry to grow Ge and SiGe epilayers and it is relatively low cost. Although the first results have been very encouraging, there are hurdles to overcome. The epitaxial growth of $Ge_{1-x}Sn_x$ requires very low temperatures otherwise the Sn is unstable and leads to segregation, thus growth temperatures are typically below 300 °C–350 °C depending on method of temperature measurements in particular CVD system [1, 2, 5, 9, 12]. As it is more reactive, Ge_2H_6 is a more favourable precursor than GeH_4 at this temperature.

In this work, heteroepitaxy of $Ge_{1-x}Sn_x$ on Si (001) substrates, via relaxed Ge buffer, has been studied using both Ge precursors, GeH_4 and Ge_2H_6 with $SnCl_4$ for a direct comparison. Their effects on epilayer quality and mechanisms of Sn incorporation into $Ge_{1-x}Sn_x$ have been researched.

2. Experimental details

$Ge_{1-x}Sn_x$ epilayers for this work were grown within an ASM Epsilon 2000 industrial type reduced pressure chemical vapour deposition (RP-CVD) system. All epilayers were grown on 100 mm diameter Si (001) substrates via a relaxed Ge buffer with thickness ~1.2 μm. $SnCl_4$ was used as a Sn precursor while either GeH_4 or Ge_2H_6 was used as the Ge precursor. Growth was carried out at different temperatures between 250 °C and 350 °C in a H_2 carrier gas and at reduced pressures below 100 Torr. For each experiment, all growth parameters were chosen to achieve similar $Ge_{1-x}Sn_x$ epilayers by means of GeH_4 or Ge_2H_6 precursors. Partial pressure for GeH_4 or Ge_2H_6 was fixed at 20 mTorr and 10 mTorr, respectively, and for $SnCl_4$ it was varied from 5 to 40 mTorr. The schematic cross-section of the growth structures is shown in figure 1.

Sn content in $Ge_{1-x}Sn_x$ epilayers, their thicknesses and surface morphology were characterised by a variety of techniques. Epilayer thickness uniformity was mapped across the wafers using Fourier transform infrared spectroscopy (FTIR) reflectance measurements. This was carried out within a Bruker Vertex v70 FTIR with a MappIR accessory capable of mapping across wafers up to 200 mm in diameter.

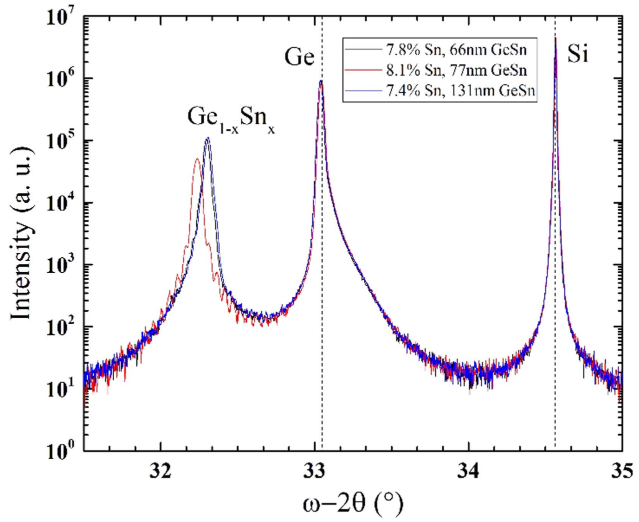

Figure 2. HR-XRD coupled scans for $Ge_{1-x}Sn_x$ grown by 10 mTorr Ge_2H_6 at temperature of 270 °C with $SnCl_4$ partial pressure of 5 mTorr, 10 mTorr and 15 mTorr for the samples with 7.8%, 8.1% and 7.4% Sn content in $Ge_{1-x}Sn_x$, respectively. The Sn content for each sample was measured from RSMs and the modified Vegard's Law. The $Ge_{1-x}Sn_x$ thicknesses were estimated from thickness fringes of HR-XRD coupled scans and then confirmed by XTEM.

High resolution x-ray diffraction (HR-XRD) was used to study the crystalline quality as well as to obtain the state strain and Sn content in the $Ge_{1-x}Sn_x$ epilayers. This was carried out via ω–2θ coupled scans for strained epilayers and symmetric and asymmetric reciprocal space maps (RSMs) on a Panalytical X'Pert Pro MRD using Cu$K\alpha_1$ source.

A Jeol JEM-2100 transmission electron microscope (TEM) was used to obtain high resolution cross-sectional micrographs of the heterostructures. TEM imaging allows direct observation of the crystalline quality (defect imaging) and measurements of an epilayer's thickness.

The surface morphology of the heterostructures was mapped using an Asylum Research MFP-3D stand-alone atomic force microscope (AFM). The surface topology and roughness were captured using Silicon Nitride (Si_3N_4) tips on the AFM operating in tapping mode.

Precipitants on the surface of the $Ge_{1-x}Sn_x$ were analysed by using a Zeiss SUPRA 55-VP scanning electron microscope (SEM) with a field emission electron gun (FEG). The system is equipped with an EDAX energy-dispersive x-ray spectrometer (EDS) which could be used to obtain elemental composition analysis with a detection limit of approximately 0.5 at%.

3. Results and discussion

The HR-XRD coupled scans for epi-wafers grown by Ge_2H_6 and GeH_4 are shown in figures 2 and 3, respectively. As it can be seen in these figures, the peaks at ~34.6° and ~33.0° are originated from Si (001) substrate and Ge buffer layer,

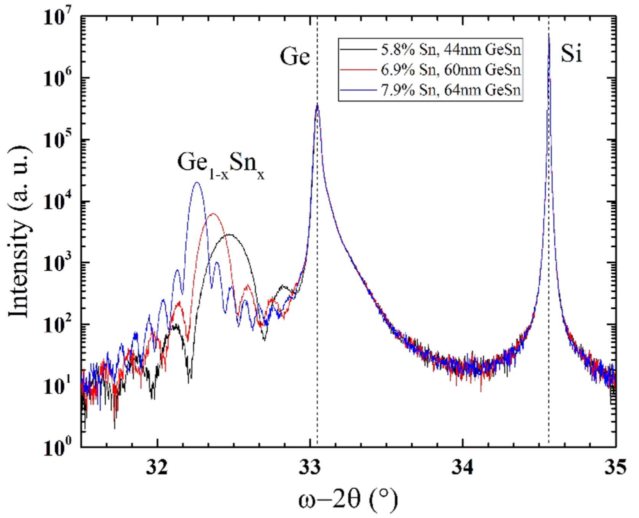

Figure 3. HR-XRD coupled scans for $Ge_{1-x}Sn_x$ grown by 10 mTorr GeH_4 at temperature of 280 °C with $SnCl_4$ partial pressure of 10 mTorr, 20 mTorr and 40 mTorr for the samples with 5.8%, 6.9% and 7.9% Sn content in $Ge_{1-x}Sn_x$, respectively. The Sn content for each sample was measured from RSMs and the modified Vegard's Law. The $Ge_{1-x}Sn_x$ thicknesses were estimated from thickness fringes of HR-XRD coupled scans and then confirmed by XTEM.

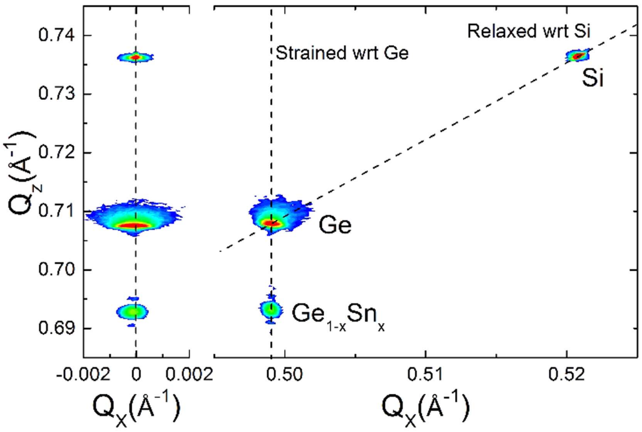

Figure 4. Symmetric (left) and asymmetric (right) RSMs of a fully strained $Ge_{0.919}Sn_{0.081}$ layer is grown on a relaxed Ge buffer on a Si (001) substrate.

respectively. There are also strong peaks between 32° and 33° indicating the successful growth of $Ge_{1-x}Sn_x$ epilayers using both precursors, however, the shift in the Bragg peaks to lower angles in figure 2 demonstrates higher Sn incorporation. Thickness fringes can be observed in of the spectra and are a result of x-ray interference from fully strained epilayers, which can be used to calculate epilayer's thickness.

A typical symmetrical and asymmetrical RSM of a strained ~131 nm thick $Ge_{0.919}Sn_{0.081}$ on Ge/Si (001) virtual substrate is shown in figure 4. The (004) Bragg peaks are aligned in the in-plane reciprocal coordinate (Q_x) confirming the absence of tilt in the epilayers. The asymmetric (224) RSM shows that the Ge epilayer is almost fully relaxed to the Si substrate while the $Ge_{1-x}Sn_x$ epilayer is fully strained to the Ge buffer, see figure 4. The Sn content of the epilayers is

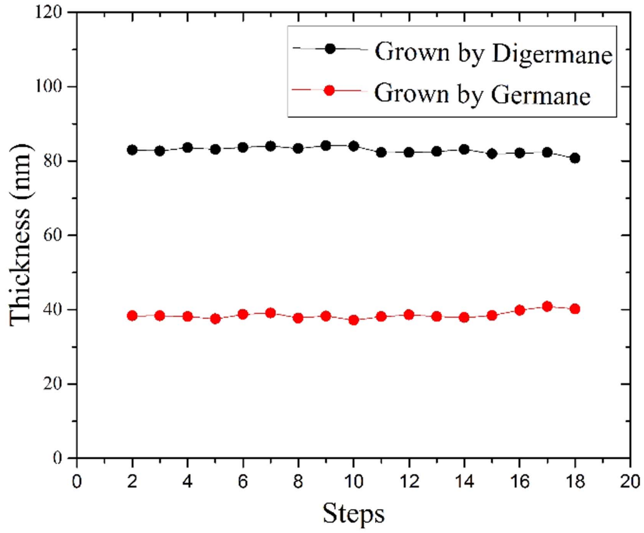

Figure 5. The thickness uniformity of two $Ge_{1-x}Sn_x$ epilayers with highest Sn content grown by Ge_2H_6 and GeH_4 precursors by FTIR.

calculated using the modified Vegard's law:

$$a_0^{Ge_{1-x}Sn_x} = a_0^{Ge}(1-x) + a_0^{Sn}x + b^{GeSn}x(1-x), \quad (1)$$

where a_0 is the relaxed lattice constant of each crystal and b^{GeSn} is the bowing parameter [10, 13]. The bowing parameter used is 0.041 Å [1, 10, 13] and a_0 is 5.6579 Å and 6.4892 Å for Ge and Sn, respectively [1]. The lattice constant of each epilayer was calculated from the in and out of plane lattice parameters obtained from RSMs.

The thickness uniformity of epilayers across 100 mm wafer was examined by FTIR. An example of $Ge_{1-x}Sn_x$ epilayers, grown by GeH_4 and Ge_2H_6, thickness uniformity is shown in figure 5. Thickness uniformity below 5% for the wafer grown by GeH_4 and is even lower for the wafer grown by Ge_2H_6, ~2%, is obtained. For thin $Ge_{1-x}Sn_x$ epilayers, i.e. below 100 nm, the accuracy of an epilayer thickness measured by FTIR is limited and therefore, the thicknesses of thin $Ge_{1-x}Sn_x$ epilayers were obtained more accurately with the help of XRD and XTEM measurements.

The thicknesses of these layers were more accurately measured using XTEM. The micrograph shown on the right in figure 6 shows a typical XTEM (004) image of the Ge buffer and $Ge_{0.919}Sn_{0.081}$ epilayer grown on the Si (001) substrate. The thickness of the Ge buffer layer is ~1.4 μm and the thickness of $Ge_{0.919}Sn_{0.081}$ is ~131 nm. TEM is a key technique to study the quality of the $Ge_{1-x}Sn_x$ epilayers. The defects, surface precipitation and dislocations were all studied by means of XTEM. Figure 7 shows the lattice resolution of Ge–$Ge_{0.919}Sn_{0.081}$ interface. As seen in figure 7, the XTEM image, which was obtain in (224) condition, the $Ge_{1-x}Sn_x$/Ge interface is sharp and defect-free. It can be seen clearly that $Ge_{0.919}Sn_{0.081}$ is fully strained and no dislocations are observed. Also, the precipitation on the surface, above $Ge_{0.919}Sn_{0.081}$ layer can be studied by TEM, as shown in figure 8, however, either increasing Sn content in the $Ge_{1-x}Sn_x$ epilayer or its thickness leads to degradation of epilayer quality and surface morphology. Both affects appear

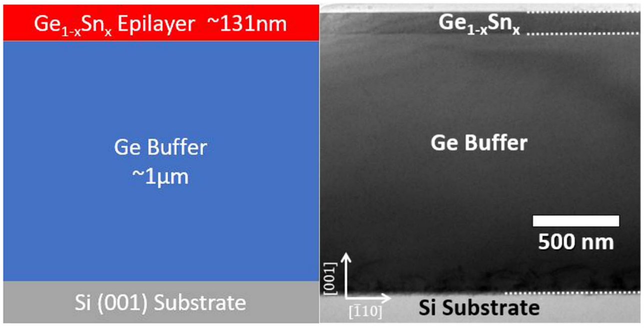

Figure 6. Left: The structure of layers. Right: TEM image of Si–Ge–$Ge_{0.919}Sn_{0.081}$ interface (straight through with 12 000X magnification, 200 KeV), with Ge buffer ~1.4 μm, $Ge_{0.919}Sn_{0.081}$ ~131 nm. The epilayer was grown by means of Ge_2H_6 (10 mTorr) and $SnCl_4$ (15 mTorr) at the temperature of 270 °C.

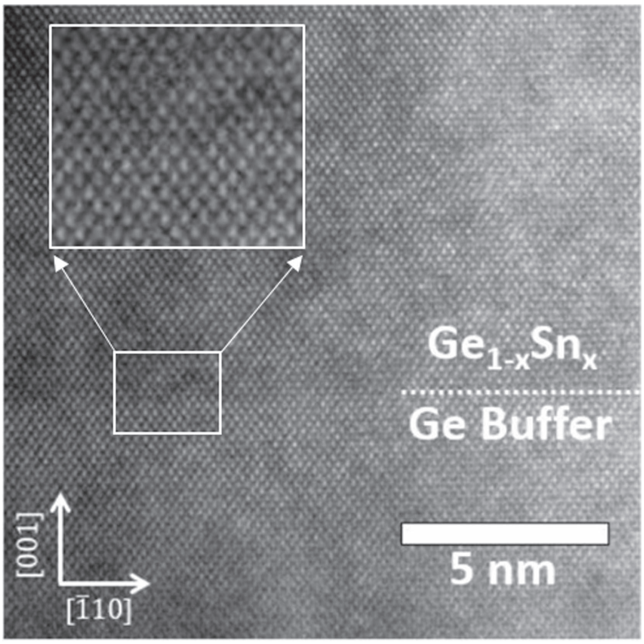

Figure 7. Lattice resolved XTEM micrograph at the Ge–$Ge_{0.919}Sn_{0.081}$ interface. The condition of XTEM: straight through with 500 000X magnification, 200 KeV. The epilayer was grown by means of Ge_2H_6 (10 mTorr) and $SnCl_4$ (15 mTorr) at the temperature of 270 °C.

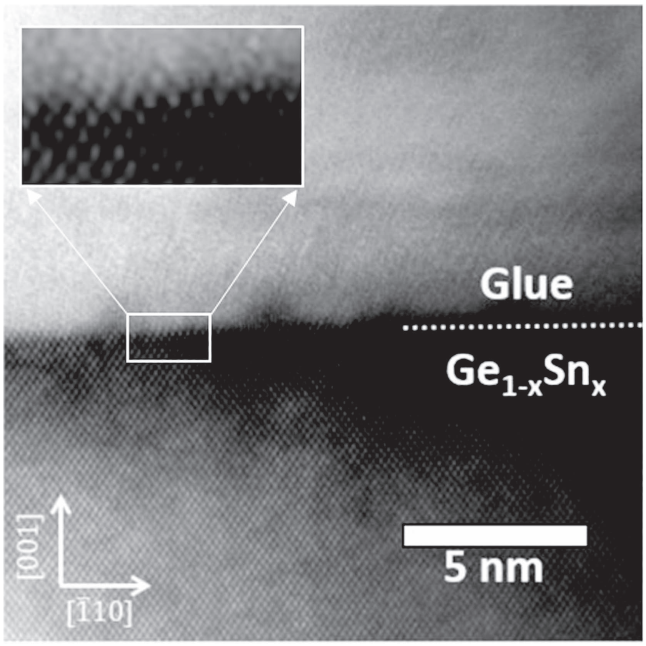

Figure 8. Lattice resolved XTEM micrograph of $Ge_{0.919}Sn_{0.081}$ surface, showing precipitation. The condition of XTEM: straight through with 500 000X magnification, 200 KeV. The epilayer was grown by means of Ge_2H_6 (10 mTorr) and $SnCl_4$ (15 mTorr) at the temperature of 270 °C.

as a consequence of Sn segregation. As GeH_4 precursor is more cost effective, it is more favourable than Ge_2H_6 precursor.

The surface roughness of three $Ge_{1-x}Sn_x$ epilayers grown with the same conditions and different $SnCl_4/H_2$ partial pressure are shown in figure 9. They are all grown by Ge_2H_6 precursor and as can be seen in the AFM scans, the surface roughness increases with increasing $SnCl_2/H_2$ partial pressure and consequently increasing Sn content in the $Ge_{1-x}Sn_x$ epilayer due to the precipitation of the Sn on the surface of the fully strained epilayer. However, in the case of using GeH_4 precursor, the surface roughness remains as low as ~0.9 nm.

The structures appeared on the $Ge_{1-x}Sn_x$ surfaces as a consequence of the Sn segregation were studied by SEM equipped with EDAX energy-dispersive x-ray (EDS) spectrometer to analyse elemental composition on the samples' surfaces. The EDS scan of $Ge_{0.919}Sn_{0.081}$ is given in figure 10. For the sample with highest surface roughness of 3 nm ($Ge_{0.926}Sn_{0.074}$) the EDS surface scans are presented in figure 11. As it can be seen, due to Sn segregation, the Sn structures appears on the $Ge_{1-x}Sn_x$ surface as the Sn concentration and partial pressure increases.

All compressive strained $Ge_{1-x}Sn$ epilayers grown by GeH_4 have low surface roughness of less than 1 nm. They replicate the surface morphology of the underlying relaxed Ge buffer which exhibits very smooth surface with rms surface roughness of just less than ~1 nm. It can be seen in figure 12, as the $SnCl_4/H_2$ partial pressure increases when GeH_4 is used as precursor, the surface roughness remains low, in other words, the Sn precipitation is being controlled by means of GeH_4. This is very important when thicker $Ge_{1-x}Sn_x$ epilayer is required to be grown.

For either GeH_4 or Ge_2H_6 precursors, the higher Sn content in a $Ge_{1-x}Sn_x$ epilayer can be achieved by decreasing the temperature, [1, 7] as long as the precursors are still reactive at such low temperatures. For instance, as the growth temperature decreases from 280 °C to 275 °C for those samples grown by GeH_4, the Sn content in $Ge_{1-x}Sn_x$ was increased by 1%. It is important to understand that one of the consequences of decreasing temperature is lowering the growth rate. This also has been observed in our research. The results show that the Sn content in $Ge_{1-x}Sn_x$ increases as the $SnCl_4$ partial pressure increases up until a certain level where increasing in $SnCl_4$ partial pressure results in decreasing the Sn content in $Ge_{1-x}Sn_x$. Results of it are shown in figures 10 and 11. One of the reasons can be the fact that higher $SnCl_4$

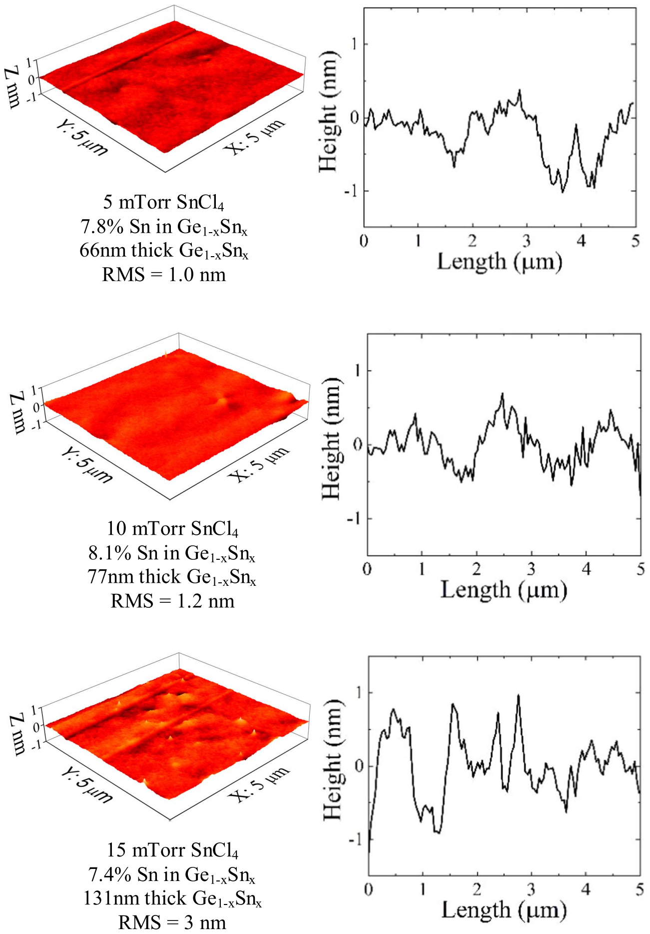

Figure 9. Left: 3D AFM scans with surface roughness measured by tapping mode AFM for the wafers grown by Ge_2H_6, at the temperature of 270 °C with different $SnCl_4/H_2$ partial pressure. Right: Align profile through the centre of each AFM scan. As the $SnCl_4/H_2$ partial pressure increases, the Sn segregation happens resulting increasing the surface roughness (rms). These rms's were measured from 20 μm × 20 μm scan.

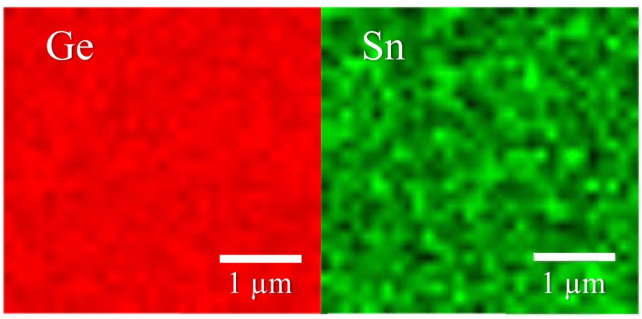

Figure 10. EDS scan of $Ge_{0.919}Sn_{0.081}$ epilayer grown by 10 mTorr Ge_2H_6 precursor with 5 mTorr $SnCl_4$ partial pressure with 1.0 nm rms and 66 nm thick epilayer. Left: Ge (GeL emission line) Right: Sn (SnL emission line).

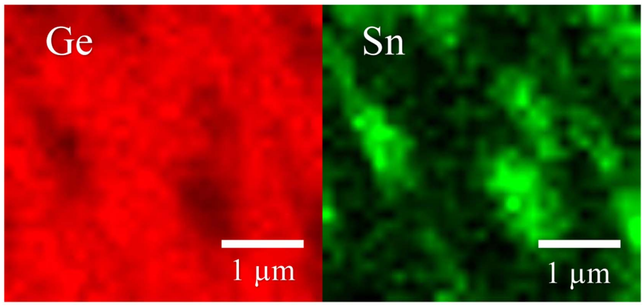

Figure 11. EDS scan of $Ge_{0.926}Sn_{0.074}$ epilayer grown by 10 mTorr Ge_2H_6 precursor with 15 mTorr $SnCl_4$ partial pressure with 3 nm rms and 131 thick $Ge_{1-x}Sn_x$ epilayer. Left: Ge (GeL emission line) Right: Sn (SnL emission line).

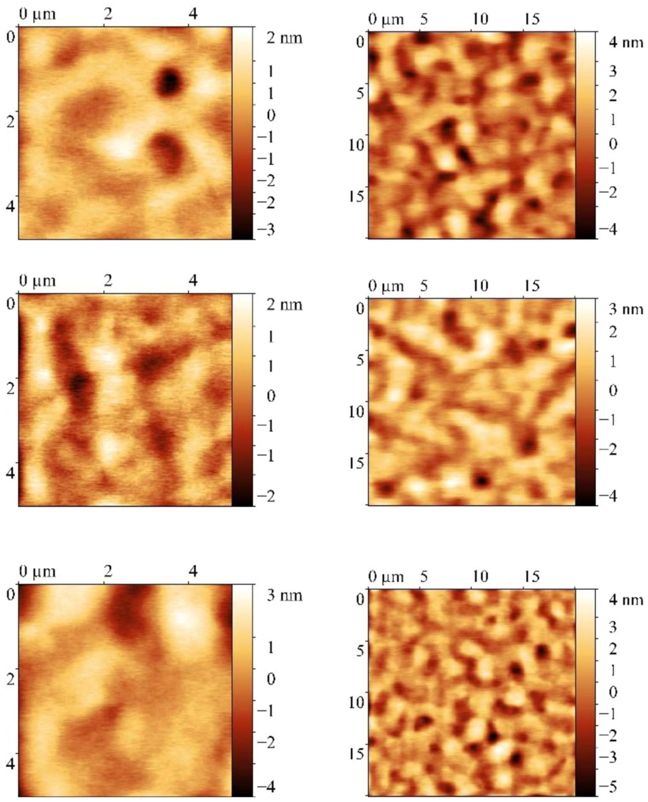

Figure 12. AFM scans of $Ge_{1-x}Sn_x$ grown by 10 m Torr GeH_4 in RP-CVD at the temperature of 280 °C. Top: AFM scans of $Ge_{1-x}Sn_x$ with 5.8% Sn in 44 nm thick $Ge_{1-x}Sn_x$ (10 mTorr $SnCl_4$ partial pressure) with surface roughness of 0.8 nm. Middle: AFM scans of $Ge_{1-x}Sn_x$ with 6.9% Sn in 66 nm thick $Ge_{1-x}Sn_x$ (15 mTorr $SnCl_4$ partial pressure) with surface roughness of 0.8 nm. Bottom: AFM scans of $Ge_{1-x}Sn_x$ (15 mTorr $SnCl_4$ partial pressure) with 7.9% Sn in 64 nm thick $Ge_{1-x}Sn_x$ with surface roughness of 0.9 nm. As the $SnCl_4/H_2$ partial pressure increases, the Sn content in $Ge_{1-x}Sn_x$ epilayer increases and the surface roughness remains low.

partial pressure leads to Sn segregation resulting in contamination of the surface. Beyond this point the Sn content in the $Ge_{1-x}Sn_x$ epilayer decreases, due to the Sn precipitation of the surface. It is important to identify such critical point for particular growth conditions in order to maintain high growth rate and high Sn content with low surface roughness. Understanding such limitation can open a new path to reach high quality $Ge_{1-x}Sn_x$ with high Sn content with a practical growth rate. Our research shows that the fully strained $Ge_{1-x}Sn_x$ epilayers grown by GeH_4 maintain smooth surface with low surface roughness: $\leqslant$1 nm. The surface roughness of three $Ge_{1-x}Sn_x$ epilayers grown with the same growth conditions and different $SnCl_4$ partial pressures are shown in figure 9. These AFM scans confirm the presence of Sn segregation due to the high $SnCl_4$ partial pressure.

By using $SnCl_4$ and Ge_2H_6 precursors, very high Sn content (up to ~14%) can be achieved for relaxed epilayers. [1] Higher Sn incorporation is achieved by reduction of growth temperature and by suppression of Sn segregation. Moreover, higher temperatures are required to grow $Ge_{1-x}Sn_x$ epilayers when using GeH_4 as opposed to Ge_2H_6 precursor. This is simply because the GeH_4 is less reactive and thus requires higher temperatures for its bonding energy to be broken in addition to chemical reaction occurring in contact with $SnCl_4$.

In order to achieve indirect-to-direct bandgap transition in a $Ge_{1-x}Sn_x$ epilayer, the Sn content in relaxed $Ge_{1-x}Sn_x$ needs to be just over 9% [1–5]. Further process optimisation is required to achieve such high levels of Sn incorporation in the $Ge_{1-x}Sn_x$ epilayers, which could be achieved by fine tuning the $SnCl_4$ partial pressure and reducing the growth temperature. Considering the cost efficiency and availability of GeH_4 precursor, this source is more favourable compared with Ge_2H_6. Moreover, by using GeH_4 precursor, high quality $Ge_{1-x}Sn_x$ epilayers can be grown, with fewer defects and lower surface roughness compared with those of grown by Ge_2H_6 precursor at similar Sn content levels. One possible explanation for this is due to the increased purity of GeH_4 or the degradation of the Ge_2H_6 source over longer-term storage. As the chance of having Sn segregation on the surface is less in the GeH_4 case, thicker $Ge_{1-x}Sn_x$ epilayer can be grown by means of this precursor, however this has to be confirm in further research. In both cases of Ge_2H_6 and GeH_4, reducing temperature, increases the Sn incorporation in the $Ge_{1-x}Sn_x$ epilayers, however, it can reduce the growth rate significantly. [1, 7] In our research, it has been observed that reducing growth temperature from 280 °C to 275 °C results in increasing Sn incorporation by 1%. Reducing the growth further will eventually lead to a drop in Sn incorporation as the Ge precursors become unreactive, however, this limit was not reached at the lowest temperatures of this investigation (~260 °C). Another objective of $Ge_{1-x}Sn_x$ growth is to find the best RP-CVD growth conditions in order to achieve high quality $Ge_{1-x}Sn_x$ epilayers with the highest possible growth rate without flowing unreacted precursors, to increase commercial viability. It should be noted that the temperature required to grow $Ge_{1-x}Sn_x$ epilayer with GeH_4 is higher than Ge_2H_6. The growth rate achieved of $Ge_{1-x}Sn_x$ epilayer grown by GeH_4 was found to be twice as slow as using Ge_2H_6; However, the advantage of using GeH_4, is that $Ge_{1-x}Sn_x$ epilayers achieved by this precursor have relatively better quality and the Sn precipitation is also minimised.

4. Conclusions

$Ge_{1-x}Sn_x$ epilayers growth by RP-CVD using Ge_2H_6 and GeH_4 precursors have been compared. The results show that lower growth rate is achieved in $Ge_{1-x}Sn_x$ epilayers when grown using GeH_4 at the growth conditions as for those samples grown by Ge_2H_6. Lower surface roughness is observed for equivalent $Ge_{1-x}Sn_x$ epilayers grown by GeH_4 than with Ge_2H_6, a result of less Sn precipitation. This is important for achieving high quality metal contacts to the layers, further heteroepitaxial growth of multilayers and quantum wells and allows one to grow thicker $Ge_{1-x}Sn_x$ epilayers. The result of this investigation show GeH_4 could be a viable precursor choice for low cost heteroepitaxy of $Ge_{1-x}Sn_x$ epilayers.

ORCID iDs

Pedram Jahandar https://orcid.org/0000-0002-5995-1252

References

[1] Wirths S, Buca D and Mantl S 2016 *Prog. Cryst. Growth Charact. Mater.* **62** 1–39
[2] Soref R, Kouvetakis J and Menendez J 2007 *Mater. Res. Soc.* **958** L01–08
[3] Kasper E, Werner J, Oehme M, Escoubas S, Burle N and Schulze J 2012 *Thin Solid Films* **520** 3195–200
[4] Vincent B, Gencarelli F, Bender H, Marckeling C and Douhard B 2011 *Appl. Phys. Lett.* **99** 152103
[5] Bauer M R, Tolle J, Bungay C, Chizmeshya A V G, Smith D J, Menendez J and Kouvetakis J 2003 *Solid State Commun.* **127** 355–9
[6] Al-Kabi S *et al* 2016 *Appl. Phys. Lett.* **109** 171105
[7] Aubin J, Hartmann J M, Barnes J P, Pin J B and Bauer M 2017 *ECS J. Solid State Sci. Technol.* **6** 21–6
[8] Kouvetakis J, Menendez J and Chizmeshva A V G 2006 *Annu. Rev. Matter Res.* **36** 497–554
[9] Pezzoli F, Giorgioni A, Patchett D and Myronov M 2016 *ACS Photon. Lett.* **3** 2004–9
[10] Gencarelli F *et al* 2013 *ECS J. Solid State Sci. Technol.* **2** 134–7
[11] Wirths S *et al* 2015 *Nat. Photon.* **9** 88–92
[12] Bauer M R, Cook C S, Aella P, Tolle J, Kouvetakis J, Crozier P A, Chizmeshya A V G, Smith D J and Zollner S 2003 *Appl. Phys. Lett.* **83** 3489
[13] Gassenq A *et al* 2016 *Appl. Phys. Lett.* **109** 242107